PROCEEDINGS OF SCIENCE

Measurement of $R_2(\Delta\eta, \Delta\varphi)$ and $P_2(\Delta\eta, \Delta\varphi)$ correlation functions in pp collisions at $\sqrt{s}$ = 13 TeV with ALICE

Baidyanath Sahoo[a,*] **for the ALICE Collaboration**

[a] *Department of Physics, Indian Institute of Technology (IIT) Bombay, Mumbai, India*

E-mail: baidya@iitb.ac.in

Two-particle normalized cumulants of particle number correlations (R_2) and transverse momentum correlations (P_2), measured as a function of relative pseudorapidity and azimuthal angle difference $(\Delta\eta, \Delta\varphi)$, provide key information about particle production mechanisms, diffusivity, and conservation of charge and momentum in high-energy collisions. To complement the recent ALICE measurements in Pb–Pb collisions, as well as for better understanding of the jet contribution and nature of collectivity in small systems, these observables are measured in pp collisions at $\sqrt{s}$ = 13 TeV with similar transverse momentum range, $0.2 \leq p_{\mathrm{T}} \leq 2.0$ GeV/c. The R_2 and P_2 results on the near- and away-side are qualitatively similar, but differ quantitatively. A much narrower near-side peak is observed for P_2 compared to R_2 for both charge-independent and charge-dependent combinations, as in the recently published ALICE results for p–Pb and Pb–Pb collisions. Since these results are sensitive to the interplay between the underlying event and mini-jets in pp collisions, they not only establish a baseline for heavy-ion collisions, but also allow a better understanding of signals that are compatible with the presence of collective effects in small systems.

The Tenth Annual Conference on Large Hadron Collider Physics - LHCP2022
16-20 May 2022
online

*Speaker

© Copyright owned by the author(s) under the terms of the Creative Commons Attribution-NonCommercial-NoDerivatives 4.0 International License (CC BY-NC-ND 4.0).

https://pos.sissa.it/

PoS(LHCP2022)329

Introduction

The measurements of two- and multi-particle azimuthal correlation functions confirmed the existence of anisotropic flow (i.e., conversion of spatial anisotropies in initial conditions of the collision to momentum anisotropies of produced particles via multiple interactions) in A–A collisions at RHIC and LHC and revealed the presence of flow in smaller systems (e.g., p–A and high multiplicity pp collisions). Measurements of two-particle number correlations, R_2, and transverse momentum correlations, P_2, indicated the collective nature of the azimuthal correlations measured in Pb–Pb collisions [1]. Centrality studies in A–A collisions show that near-side peak of both charge-independent (CI) and charge-dependent (CD) correlations is narrower for P_2 than in R_2 [2]. The correlator P_2 provides a more discriminating probe of the correlation structure of jets and their underlying events than the R_2. This is further tested by measuring the R_2 and P_2 correlation functions for unidentified charged hadrons in the transverse momentum range $0.2 \leq p_{\mathrm{T}} \leq 2.0$ GeV/c in pp collisions at $\sqrt{s}$ = 13 TeV recorded by ALICE.

Correlation functions

The R_2 and P_2 correlation functions are constructed using single- and two-particle densities ($\rho_1(\eta,\varphi)$ and $\rho_2(\eta_1,\varphi_1,\eta_2,\varphi_2)$, respectively) as a function of the particle pseudorapidity (η) and the azimuthal angle (φ).

The R_2 is defined as a two-particle cumulant normalized by the product of single-particle densities as follows

$$R_2(\eta_1,\varphi_1,\eta_2,\varphi_2) = \frac{\rho_2(\eta_1,\varphi_1,\eta_2,\varphi_2)}{\rho_1(\eta_1,\varphi_1)\times\rho_1(\eta_2,\varphi_2)} - 1. \tag{1}$$

The P_2 is defined as the ratio of differential correlator $\langle\Delta p_{\mathrm{T}}\Delta p_{\mathrm{T}}\rangle$ to the square of the average transverse momentum, $\langle p_{\mathrm{T}}\rangle$, to make it dimensionless like R_2, as follows

$$\begin{aligned} P_2(\eta_1,\varphi_1,\eta_2,\varphi_2) =& \frac{\langle\Delta p_{\mathrm{T}}\Delta p_{\mathrm{T}}\rangle(\eta_1,\varphi_1,\eta_2,\varphi_2)}{\langle p_{\mathrm{T}}\rangle^2} \\ =& \frac{1}{\langle p_{\mathrm{T}}\rangle^2}\times\frac{\int_{p_{\mathrm{T,min}}}^{p_{\mathrm{T,max}}}\mathrm{dp_{T,1}dp_{T,2}}\rho_2(\mathrm{p_1,p_2})\Delta\mathrm{p_{T,1}}\Delta\mathrm{p_{T,2}}}{\int_{p_{\mathrm{T,min}}}^{p_{\mathrm{T,max}}}\mathrm{dp_{T,1}dp_{T,2}}\rho_2(\mathrm{p_1,p_2})}, \end{aligned} \tag{2}$$

where $\Delta p_{\mathrm{T,i}} = p_{\mathrm{T,i}} - \langle p_{\mathrm{T}}\rangle$ [3]. The $\langle\Delta p_{\mathrm{T}}\Delta p_{\mathrm{T}}\rangle$ correlator is positive, leading to positive value of P_2 if both particles have a larger or smaller p_{T} than the $\langle p_{\mathrm{T}}\rangle$, but it is negative if one particle has a lower and the other a larger p_{T} than the $\langle p_{\mathrm{T}}\rangle$.

For better visualization of the figures, the correlators R_2 and P_2 are convoluted from (η_1,η_2) and (φ_1,φ_2) into $\Delta\eta$ and $\Delta\varphi$, respectively and then shifted by $-\pi/2$ along $\Delta\varphi$ as follows

$$\begin{aligned} O(\Delta\eta,\Delta\varphi) = \frac{1}{\Omega(\Delta\eta)}\int & O(\eta_1,\varphi_1,\eta_2,\varphi_2)\delta(\Delta\varphi-\varphi_1+\varphi_2) \\ & \times\mathrm{d}\varphi_1\mathrm{d}\varphi_2\delta(\Delta\eta-\eta_1+\eta_2)\mathrm{d}\eta_1\mathrm{d}\eta_2, \end{aligned} \tag{3}$$

where $\Omega(\Delta\eta)$ represents the width of the acceptance in $\bar{\eta} = (\eta_1+\eta_2)/2$ at a given value of $\Delta\eta$ [4].

PoS(LHCP2022)329

The analysis of the R_2 and P_2 correlation functions are carried out for charge combination pairs $(+-)$, $(-+)$, $(++)$, and $(--)$ to yield charge-independent, $O^{\mathrm{CI}} = \frac{1}{2}[O^{+-} + O^{++} + O^{-+} + O^{--}]$, and charge-dependent, $O^{\mathrm{CD}} = \frac{1}{2}[O^{+-} - O^{++} + O^{-+} - O^{--}]$, correlation functions [5].

Results

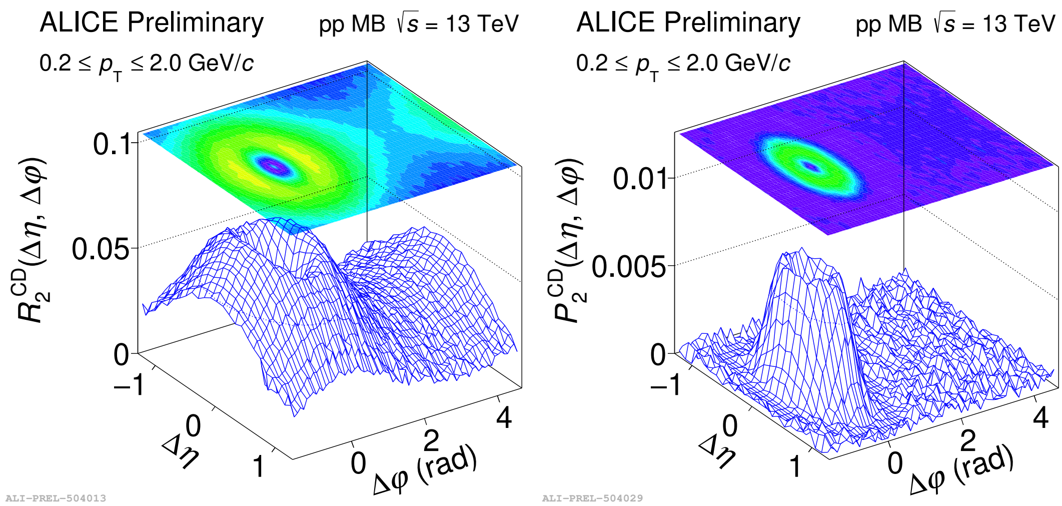

Figure 1: Correlation functions R_2^{CD} (left panel) and P_2^{CD} (right panel) of charged hadrons obtained in the selected p_{T} range in pp collisions at $\sqrt{s}$ = 13 TeV.

The R_2 and P_2 correlation functions for CD charge combinations are shown in the left and right panels of Fig. 1, respectively. Due to Hunbary-Brown Twiss (HBT) effect, both R_2^{CD} and P_2^{CD} have a dip around $(\Delta\eta, \Delta\varphi) = (0, 0)$. The away-side of R_2^{CD} features a saddle-shape structure, whereas P_2^{CD} has a flat away-side.

Note that the R_2^{CD} correlation function is related to the charge balance function, so the width of the near-side peak provides information about the balance function. Figure 2 shows the width of CD pairs of R_2 and P_2 correlation functions along $\Delta\varphi$ measured within $|\Delta\eta| \leq 1.6$ in pp, p–Pb, and Pb–Pb collisions as a function of average charged-particle multiplicity density. The widths of R_2^{CD} and P_2^{CD} vary with centrality due to radial flow and diffusivity in Pb–Pb collisions. The widths of R_2^{CD} decrease in p–Pb collisions, while the widths of P_2^{CD} show the opposite trend. The P_2^{CD} has a smaller width than the R_2^{CD}, which is due to the *angular ordering* [6] of the p_{T} of the jet constituents. The widths of $R_2^{\mathrm{CD}}(\Delta\varphi)$ and $P_2^{\mathrm{CD}}(\Delta\varphi)$ in pp collisions show good agreement with the peripheral p–Pb collisions.

In Fig. 3, the widths along $\Delta\eta$ increase monotonically from peripheral to central collisions for both $R_2^{\mathrm{CI}}(\Delta\eta)$ and $P_2^{\mathrm{CI}}(\Delta\eta)$. There is an exception for $P_2^{\mathrm{CI}}(\Delta\eta)$ for the peripheral collisions. This trend in $R_2^{\mathrm{CI}}(\Delta\eta)$ and $P_2^{\mathrm{CI}}(\Delta\eta)$ is due to anisotropic flow in Pb–Pb collisions. The widths exhibit a weak dependence in the p–Pb case. The widths of pp collisions have similar magnitude to those measured in p–Pb collisions.

PoS(LHCP2022)329

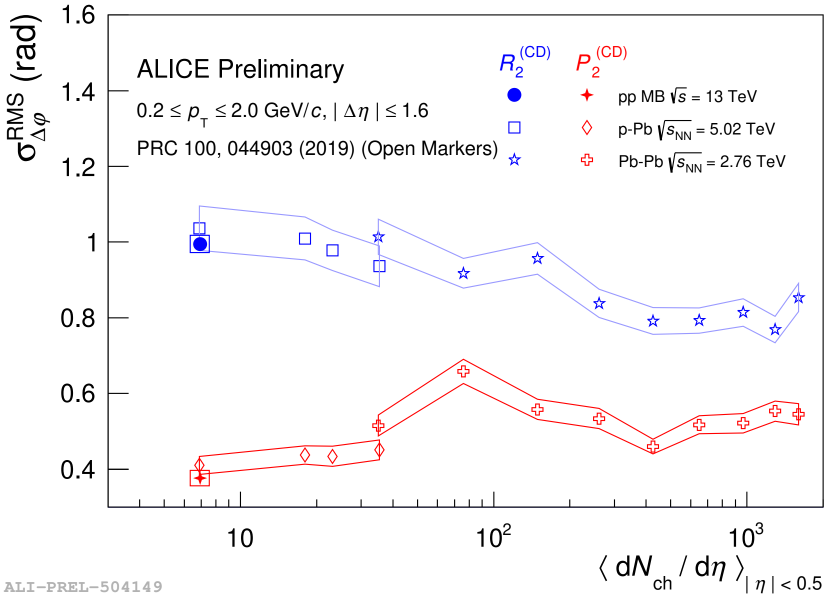

Figure 2: The widths of $R_2^{CD}(\Delta\varphi)$ (blue markers) and $P_2^{CD}(\Delta\varphi)$ (red markers) correlation functions along $\Delta\varphi$ measured within $|\Delta\eta| \leq 1.6$ in pp, p–Pb, and Pb–Pb collisions as a function of $\langle dN_{ch}/d\eta\rangle_{|\eta|<0.5}$. Vertical bars and lines represent statistical and systematic uncertainties, respectively.

Summary

The two-particle correlation functions $R_2(\Delta\eta, \Delta\varphi)$ and $P_2(\Delta\eta, \Delta\varphi)$ have been measured in pp collisions at $\sqrt{s} = 13$ TeV recorded by ALICE. The measurements were carried out using unidentified charged hadrons in the p_T range of 0.2–2.0 GeV/c. The R_2 and P_2 correlation functions for the charge-dependent combination exhibit a dip around $(\Delta\eta, \Delta\varphi) = (0, 0)$, which is largely due to HBT correlations. It is observed that the width of the near-side peak of the P_2 is significantly narrower than the near-side peak of the R_2, which is due to the angular and transverse momentum ordering. The widths of the charge-independent and charge-dependent of R_2 and P_2 correlation functions are compared with previously published results in p–Pb and Pb–Pb collisions [2]. The widths show a consistent trend among the three collision systems.

References

[1] S. Acharya et al. (ALICE Collaboration), Phys. Rev. Lett. **118**, 162302 (2017).

[2] J. Adam et al. (ALICE Collaboration), Phys. Rev. **C100**, 044903 (2019).

[3] C. Pruneau, S. Gavin, and S. Voloshin, Phys. Rev. **C66**, 044904 (2002).

[4] M. Sharma and C. A. Pruneau, Phys. Rev. **C79**, 024905 (2009).

[5] S. Bass, P. Danielewicz and S. Pratt, Phys. Rev. Lett. **85**, 2689 (2000).

[6] B. Sahoo, B.K. Nandi, P. Pujahari, S. Basu and C. Pruneau, Phys. Rev. **C100**, 024909 (2019).

PoS(LHCP2022)329

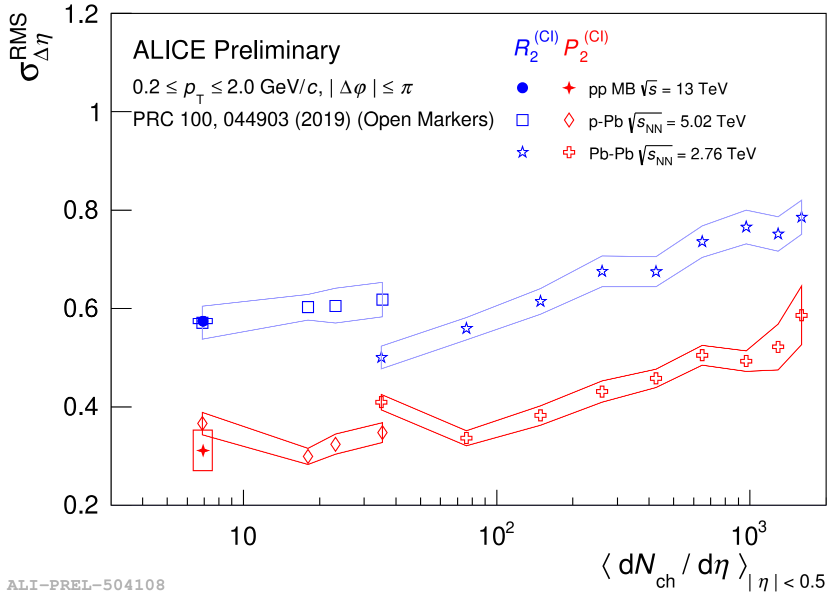

Figure 3: The widths of $R_2^{CI}(\Delta\eta)$ (blue markers) and $P_2^{CI}(\Delta\eta)$ (red markers) correlation functions along $\Delta\eta$ measured within $|\Delta\varphi| \le \pi$ in pp, p–Pb, and Pb–Pb collisions as a function of $\langle dN_{ch}/d\eta\rangle_{|\eta|<0.5}$. Vertical bars and lines represent statistical and systematic uncertainties, respectively.

PoS(LHCP2022)329